Contribution from the Extraterrestrial Research Division,
Ames Research Center, NASA, Moffett Field, California 94035

Quantum-Chemical Modeling of Smectite Clays

S. ARONOWITZ,*[1a] L. COYNE,[1a] J. LAWLESS, and J. RISHPON[1b]

Received October 16, 1981

A self-consistent charge extended Hückel program was employed to model isomorphic substitution of Al^{3+} by Na^+, K^+, Mg^{2+}, Ca^{2+}, Fe^{2+}, and Fe^{3+} in the octahedral layer of a dioctahedral smectite clay such as montmorillonite. Upon comparison of the energies involved in the isomorphic substitution, the ordering for successful substitution is $Al^{3+} > Fe^{3+} > Mg^{2+} > Fe^{2+} > Na^+ \simeq Ca^{2+} > K^+$. This ordering is consistent with experimental observation. The calculations also permitted determination of possible penetration of metal ions into the clay's 2:1 crystalline layer. For the cases studied, such penetration can occur at elevated temperatures into regions where isomorphic substitution has occurred with metal ions that bear a formal charge of less than 3+. The computed behavior of the electronic structure when there is isomorphic substitution is similar to behavior associated with semiconductors.

Introduction

The structures of the clay minerals and their identification by X-ray diffraction have been the subjects of a number of studies summarized by Brown,[2] Grim,[3] and van Olphen,[4] among others. In general, the 2:1 layer silicates share the common feature that two silica sheets sandwich a sheet of octahedrally coordinated metal ions (for the dioctahedral smectites, the principal metal ion is aluminum). A representative 2:1 layer, which also serves as the model used in the series of computations to be reported here, is displayed in Figure 1. The diversity of the members of the 2:1 layer silicates occurs because of their capacity for isomorphic substitution of various cations in the octahedral or tetrahdral layers. Substitution of a divalent metal ion (such as Mg^{2+}) for the trivalent Al^{3+} or a trivalent metal ion (Al^{3+}) for the tetravalent Si results in a net negative charge and in the interaction with positive ions (the exchangeable cations) from an interlaminar hydrated phase.[5] In this context, we have used quantum-chemial calculations to (1) evaluate the magnitude of this surface charge and (2) determine the applicability of this approach for the prediction of the preference of isomorphic substitutions among various elements.

There have been investigations on various simple silicate structures in which quantum-chemical methods were used.[6] The theoretical approach for complex clay systems, however, has been a classical one, as exemplified by Giese's work on the expandability of 2:1 clays.[7] This paper will explore a model of the critical and complex 2:1 layer with a semiempirical quantum-chemical program. The method is discussed in the next section.

Modifications to an Iterative Extended Hückel Program

The quantum-chemical program used in this report is based upon the conventional self-consistent charge extended Hückel model.[8] Modifications of the program were made in the spirit of older approaches;[9,10] they are largely incorporated in a dynamic variation of a major parameter in extended Hückel (the valence orbital ionization energy), which preserves the relative simplicity of the method. A full description of the program is presented elsewhere.[11] It has been used to successfully describe the interactions of bare and hydrated metal ions with molecules of biological interest[12] as well as the adsorption and recombination of hydrogen atoms on graphite crystals.[13]

Given that Z_i(valence) is the residual nuclear charge of the ith atomic center, which is obtained by assuming the core electrons to completely shield their counterpart of positive charge, then, between the ith and jth centers separated by a distance R_{ij}, we set

$$(Z_iZ_j)^{(l)}(\text{effective}) = [Z_i(\text{valence}) - \sum_{k(i)} P_{k(i)}(0,{}^1/_2R_{ij})\rho^{(l)}{}_{k(i)}][Z_j(\text{valence}) - \sum_{t(j)} P_{t(j)}(0,{}^1/_2R_{ij})\rho^{(l)}{}_{t(j)}] \quad (1)$$

where $P_{k(i)}[0,{}^1/_2R_{ij}]$ is the probability of finding an electron in the kth orbital on the ith atomic center in a spherical volume of radius ${}^1/_2R_{ij}$ and $P_{t(j)}[0,{}^1/_2R_{ij}]$ is defined similarly. The $\rho^{(l)}{}_{k(i)}$ is the electronic density assigned to the kth orbital after the lth iteration. The $\rho^{(l)}{}_{t(j)}$ is similarly defined with respect to the tth orbital on the jth atomic center. In the limit, as $R_{ij} \to 0$

$$(Z_iZ_j)^{(l)}(\text{effective}) \to [Z_i(\text{valence})][Z_j(\text{valence})] \quad (2a)$$

On the other hand, as $R_{ij} \to \infty$

$$(Z_iZ_j)^{(l)}(\text{effective}) \to q^{(l)}{}_iq^{(l)}{}_j \quad (2b)$$

where $q^{(l)}{}_i$ and $q^{(l)}{}_j$ are the net charges on the ith and jth atomic centers. The contribution to the total energy after the lth iteration is given by

$$E^{(l)}(\text{effective nuclear–nuclear}) = {}^1/_2\sum_{i,j}(Z_iZ_j)^{(l)}(\text{effective})/R_{ij} \quad (i \neq j) \quad (3)$$

in atomic units; $E^{(l)}$(effective nuclear–nuclear) contains approximate expressions for nuclear attraction integrals of the form $[\psi_{k(i)}|Z/R_{ij}|\psi_{k(i)}]$.

The molecular electronic environment is more directly sensed than in self-consistent extended Hückel by introducing Coulombic modifications to the valence orbital ionization energies. In this context, the normal form of the off-diagonal elements of the Hamiltonian matrix in extended Hückel contain implicit approximations to nuclear attraction integrals of the form $[\psi_{k(i)}|V(R_{ij})|\psi_{t(j)}]$. By our scheme, an electron in the kth orbital on the ith center interacts with the electronic densities assigned to the orbitals on all other centers ($j \neq i$). A set of parameters (a_{ij}), which depends only on atomic types, is formed, and its elements are determined by variational

(1) (a) NRC Senior Research Associate. (b) Current address: Department of Chemistry, Tel Aviv University, Ramat Aviv, Israel.
(2) Brown, G. "The X-Ray Identification and Crystal Structure of Clay Minerals"; Mineralogical Society: London, 1961.
(3) Grim, R. E. "Clay Mineralogy"; McGraw-Hill Book Co.: New York, 1968.
(4) van Olphen, H. "An Introduction to Clay Colloid Chemistry"; Wiley: New York, 1977.
(5) Mering, J.; Glaeser, R. *Bull. Soc. Fr. Mineral. Cristallogr.* **1954**, *77*, 519.
(6) de Jong, B. H. W. S.; Brown, G. E., Jr. *Geochim. Cosmochim. Acta* **1980**, *44*, 491. An extensive list of pertinent references is contained in this paper.
(7) Giese, R. F. *Clays Clay Miner.* **1978**, *26*, 51.
(8) Schaffer, A. M.; Gouterman, M.; Davidson, E. R. *Theor. Chim. Acta* **1972**, *30*, 9.
(9) Anderson, A. B.; Hoffmann, R. *J. Chem. Phys.* **1974**, *60*, 4271.
(10) Anderson, A. B. *J. Chem. Phys.* **1975**, *62*, 1187.
(11) Aronowitz, S. *NASA Tech. Memo.* **1980**, *NASA TM-81200*.
(12) Aronowitz, S.; MacElroy, R.; Chang, S. *NASA Tech. Memo.* **1980**, *NASA TM-81201*.
(13) Aronowitz, S.; Chang, S., manuscript in preparation.

0020-1669/82/1321-3589$01.25/0

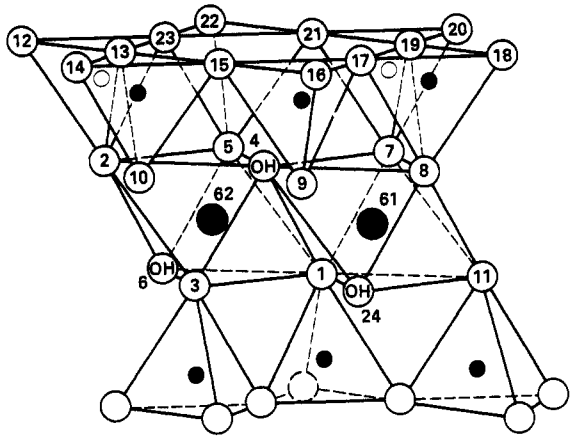

Figure 1. Structure (including unmarked atoms) used in the calculations. The open circles are oxygens, the small dark circles are silicons, and the larger dark circles are metal ions. The structure is representative of the 2:1 layer of a smectite clay (from Grim[3]).

arguments. This increment to the valence orbital ionization energy is expressed as

$$h^{(l)}_{k(l)} \equiv \sum_j \delta\epsilon^{(l)}_{k(i)j} = \sum_j a_{ij} \sum_t \rho^{(l)}_{t(j)} \int \psi_k^2 r_{k(i),t(j)}^{-1} \psi_t^2 \, d\tau \quad (4)$$

The ψ_k and ψ_t are the appropriate wave functions (in our case Slater-type functions are used). It should be noted that our treatment considers the valence orbital ionization energies to be *optimal*; that is, the set of parameters $(a_{ij}) = (0)$ unless (1) it is desired to maintain a specific value for the net charge or (2) the system exhibits instability. Since the extended Hückel theory already contains implicit two-center nuclear–electron attraction terms and we have completed the components by including the expression in eq 3, the emphasis for any variation will always reside with the Coulombic expressions. In this regard, the diagonal elements of the Hamiltonian matrix are given by

$$H^{(l)}_{k(i),k(i)} = H^{(0)}_{k(i),k(i)} + h^{(l)}_{k(i)} \qquad h^{(0)}_{k(i)} \equiv 0 \quad (5)$$

and the off-diagonal elements

$$H^{(l)}_{k(i),t(j)} = \tfrac{1}{2} K S_{k(i),t(j)} [H^{(l)}_{k(i),k(i)} + H^{(l)}_{t(j),t(j)}] \quad (6)$$

In eq 5 and 6, K is an interaction constant (set equal to 1.89 for all our calculations)[14] and $S_{k(i),t(j)}$ is the overlap between the orbitals $k(i)$ and $t(j)$. The eigenvalues of the Hamiltonian matrix may now contain two-electron contributions; however, such contributions are included in a manner that permits the energies to be treated as though they were one-electron energies. The total molecular energy after the lth iteration for an N-orbital, n-atomic-center system is given by

$$E^{(l)}_{\text{total}} = \sum_{m=1}^{N} p_m \epsilon^{(l)}_m + E^{(l)}(\text{effective nuclear–nuclear}) \quad (7)$$

The one-electron energy $\epsilon^{(l)}_m$ is associated with the mth molecular orbital, which, in turn, is occupied by p_m electrons. The first term on the right-hand side of eq 7 obeys a variational principle with respect to inclusion of electronic interaction terms; however, the $E^{(l)}_{\text{total}}$ does not, since $E^{(l)}$(effective nuclear–nuclear) may increase for incremental increases in charge separations. The energy values obtained are optimal, given the constraints of stability (no charge oscillation) and minimized electronic energies.

Finally, standard extended Hückel parameters were adopted. The appropriate valence orbital parameters for H, O, and Fe were taken from Zerner and Gouterman,[14] parameters for Mg and Ca were adopted from Zerner and Gouterman,[15] Na and K valence orbital energies were adopted from McGlynn,[16] and the corresponding ζ values were taken from Clementi and Raimondi.[17]

(14) Zerner, M.; Gouterman, M. *Theor. Chim. Acta* **1966**, *4*, 44.

Model Montmorillonite Structure

The montmorillonite structure suggested by Hofmann et al.[18] and modified by Marshall,[19] Maegdefrau and Hofmann,[20] and Hendricks[21] was adopted for our treatment. The model structure is displayed in Figure 1. It has two complete octahedral sites. The montmorillonite unit cell possesses three octahedral sites; this exceeds the iterative extended Hückel (IEH) program's present capacity. The hydrated interlaminar region also was excluded because of the same program limitation. "Dangling" bonds were not permitted; hydrogens were used to complete the unit. The basic formula for our structure is $(OH)_3M_2Si_9O_{28}$ (excluding hydrogens, of which there were 17, used to complete "dangling" bonds), where M represents metal ions in the octahedral sites. The theoretical smectite formula is $(OH)_4M_4Si_8O_{20}\cdot nH_2O$(interlayer). The mathematical model is neutral only when trivalent cations occupy both octahedral sites and all "dangling" bonds are eliminated by the binding of hydrogen.

Results

Isomorphic substitution of an Al^{3+} ion at an octahedral site by Na^+, K^+, Mg^{2+}, Ca^{2+}, Fe^{2+}, and Fe^{3+} was treated as was the case in which both octahedral sites initially were empty (each possessed a formal excess charge of 3–) followed by subsequent substitution by the above metal ions at one vacant site. No substitution of any Si in either tetrahedral layer was considered. The effects on the molecular orbitals (filled and empty) near the Fermi level are displayed in Figure 2 for the case in which Al^{3+} occupies one octahedral site and isomorphic substitution with various other cations occurs at the other site. The composition of the topmost filled molecular orbitals is not greatly affected by the specific substituent in the octahedral layer; inspection of the entries in Table I supports this claim since, with the exception of (Al^{3+},Al^{3+}), the various substitution cases show their four topmost filled MO's to be virtually localized on O3 and O6 atomic centers. Qualitatively, the filled orbitals near the Fermi level are shifted upward (destabilized) as a function of the metal ion substituent at a site; the greater the electron density transferred from the site to the metal ion, the more negative are the energies of the filled orbitals near the Fermi level. This is exemplified by the behavior of the molecular orbitals labeled A and B in Figure 2. It is noted below that the computed ordering of the magnitude of electronic density (the numbers in parentheses) transferred to the metal ion is

$$Al^{3+}(2.57) > Fe^{3+}(2.09) > Mg^{2+}(1.53) > Fe^{2+}(1.29) > Ca^{2+}(1.00) > Na^+(0.39) > K^+(0.05)$$

Thus, rather than the formal charges associated with the various cations, the calculated in situ net charges are given by 0.43+, 0.91+, 0.47+, 0.71+, 1.00+, 0.61+, and 0.95+,

(15) Zerner, M.; Gouterman, M. *Theor. Chim. Acta* **1967**, *8*, 26.
(16) McGlynn, S. P.; Vanquickenborne, L. G.; Kinoshita, M.; Carroll, D. G. "Introduction to Applied Quantum Chemistry"; Holt, Rinehart and Winston: New York, 1972.
(17) Clementi, E.; Raimondi, D. L. *J. Chem. Phys.* **1963**, *38*, 2686.
(18) Hofmann, U.; Endell, K.; Wilm, D., *Z. Kristallogr., Kristallgeom., Kristallphys., Kristallchem.* **1933**, *86*, 340.
(19) Marshall, C. E. *Z. Kristallogr., Kristallgeom., Kristallphys., Kristallchem.* **1935**, *91*, 433.
(20) Maegdefrau, E.; Hofmann, U. *Z. Kristallogr., Kristallgeom., Kristallphys., Kristallchem.* **1937**, *98*, 299.
(21) Hendricks, S. B. *J. Geol.* **1942**, *50*, 276.

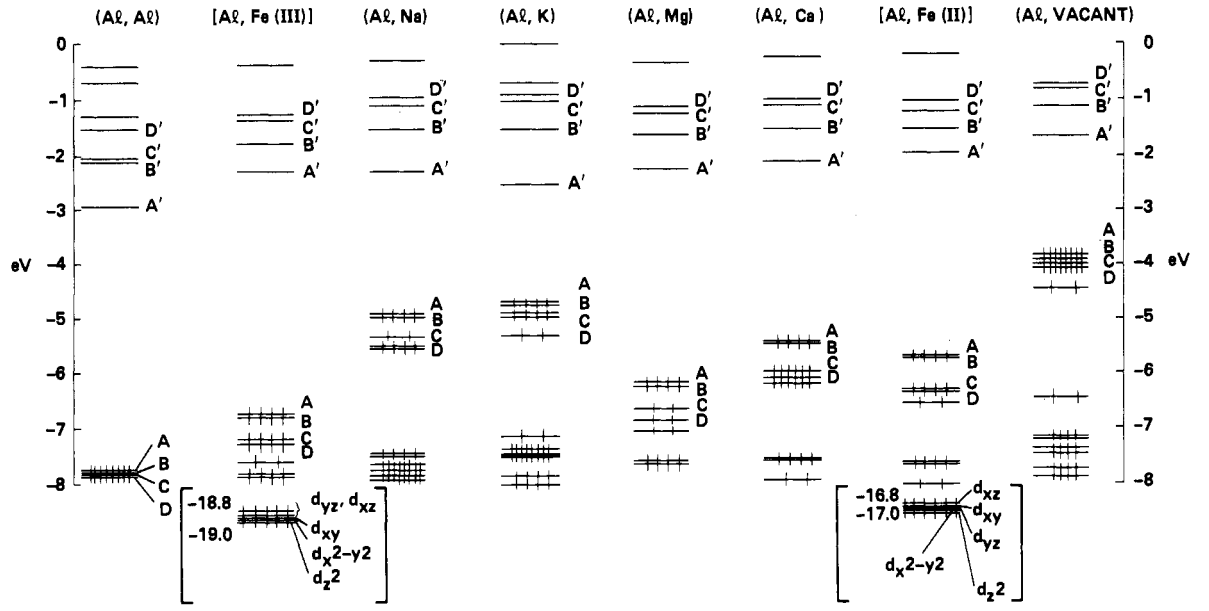

Figure 2. Behavior of the molecular orbitals near the Fermi level as a result of isomorphic substitution. The headings at the top of the figure denote the occupancy of the two octahedral sites in the 2:1 layer displayed in Figure 1. The labels D, C, B, and A denote the four topmost filled molecular orbitals (in that order) for any system, and A′, B′, C′, and D′ are the four lowest empty orbitals (in that order) for any system. The insets under [Al,Fe(III)] and [Al,Fe(II)] at the bottom of the figure display the molecular orbitals whose components are (almost) exclusively d orbitals from the iron.

Table I. Percent Composition[a] of the Four Topmost Filled and Four Lowest Empty Molecular Orbitals

cations in the pair of octahedral sites	topmost filled orbitals				lowest empty orbitals			
	D	C	B	A	A′	B′	C′	D′
(Al^{3+},Al^{3+})	O3 (58)	O3 (22)	O3 (25)	O3 (51)	Al61 (22)	Al61 (27)	Al61 (17)	Al61 (24)
	O11 (18)	O11 (54)	O11 (61)	O11 (31)	Al62 (22)	Al62 (15)	Al62 (30)	Al62 (21)
(Al^{3+},Fe^{3+})	O3 (31)	O3 (22)	O3 (81)	O3 (31)	O4 (15)	O1 (9)	O11 (18)	O24 (13)
	O6 (53)	O6 (72)	O6 (8)	O6 (53)	Al61 (29)	Al61 (39)	Al61 (43)	Al61 (56)
(Al^{3+},Na^{+})	O3 (31)	O6 (95)	O3 (86)	O3 (81)	O4 (11)	O1 (12)	O4 (14)	O8 (9)
	O6 (61)		O6 (5)	O6 (12)	Al61 (25)	Al61 (41)	Al61 (50)	Al61 (59)
(Al^{3+},K^{+})	O3 (36)	O3 (21)	O3 (67)	O3 (57)	Al61 (21)	O1 (10)	O4 (14)	O1 (8)
	O6 (56)	O6 (74)	O6 (25)	O6 (39)	K62 (10)	Al61 (40)	Al61 (41)	Al61 (57)
(Al^{3+},Mg^{2+})	O3 (41)	O3 (8)	O3 (79)	O3 (87)	Al61 (28)	O1 (10)	O11 (14)	O24 (12)
	O6 (42)	O6 (89)	O6 (12)	O6 (5)	Mg62 (11)	Al61 (39)	Al61 (51)	Al61 (55)
(Al^{3+},Ca^{2+})	O3 (59)	O3 (10)	O3 (82)	O3 (86)	O4 (13)	O1 (12)	O11 (13)	O8 (10)
	O6 (25)	O6 (87)	O6 (10)	O6 (6)	Al61 (27)	Al61 (40)	Al61 (47)	Al61 (58)
(Al^{3+},Fe^{2+})	O3 (11)	O3 (56)	O3 (81)	O3 (11)	O4 (12)	O11 (16)	O4 (14)	O8 (9)
	O6 (82)	O6 (30)	O6 (10)	O6 (82)	Al61 (30)	Al61 (39)	Al61 (46)	Al61 (57)
(Al^{3+},vacant)	O3 (29)	O3 (8)	O3 (81)	O3 (68)	O4 (13)	O11 (15)	O7 (6)	O4 (13)
	O6 (66)	O6 (90)	O6 (11)	O6 (28)	Al61 (29)	Al61 (40)	Al61 (62)	Al61 (62)

[a] Based on Mulliken population analysis. Only the two largest contributors are listed. The percentages are enclosed in the parentheses. Atom numbers correspond to the notation in Figure 1 while orbital designation corresponds to the convention used in Figure 2.

where the same cation order as in the above set of inequalities has been kept. The *same* ordering is obtained when the energy change of incorporating a metal ion into an empty octahedral site is computed. The results of these calculations are presented in Table II. It is the shift of electronic density from the octahedral layer to the particular metal ion that will determine the degree of stability in the isomorphically substituted structure. In the case when that ion is K^+, for example, the configuration is actually destabilized with respect to a vacancy (see Table II). [A more realistic process than that considered in Table II is

$$(Al^{3+},\text{vacant})^{3-}(\text{clay}) + M^{i+}(\text{aq}) \rightarrow (Al^{3+},M^{i+})^{i-3}(\text{clay}) + H_2O$$

Modeling this reaction exceeds the capabilities of the IEH program.] It is interesting to note that this ordering agrees with the one Goldschmidt[22] proposed. His proposal was based on the approximate relative sizes of metal ions at their appropriate valencies. Octahedral substitutions by Na^+, K^+, and

Table II. Isomorphic Substitutions in the Smectite Structure

M^{i+}	ΔE_1 [$(Al^{3+},\text{vacant})^{3-}$ + $M^{i+} \rightarrow (Al^{3+},M^{i+})^{i-3}$], eV	ΔE_2 [$(\text{vacant},\text{vacant})^{6-}$ + $M^{i+} \rightarrow (M^{i+},\text{vacant})^{i-6}$], eV
Na^+	−9.3	−30.8
K^+	+7.3	−12.6
Mg^{2+}	−40.0	−79.2
Ca^{2+}	−8.7	−49.2
Fe^{2+}	−27.4	−66.7
Al^{3+}	−77.6	−129.8
Fe^{3+}	−46.9	−104.8

Ordering (Most Favored Cation Substituent to least Favored)

$Al^{3+} > Fe^{3+} > Mg^{2+} > Fe^{2+} > Na^+ \simeq Ca^{2+} > K^+$ $\quad$ $Al^{3+} > Fe^{3+} > Mg^{2+} > Fe^{2+} > Ca^{2+} > Na^+ > K^+$

Miscellaneous Reaction

$$(Al^{3+},Fe^{3+})^0 + e^- \rightarrow (Al^{3+},Fe^{2+})^- \quad \Delta E = +4.4 \text{ eV}$$

(22) Goldschmidt, V. M. *Skr. Nor. Vidensk.-Akad. [Kl.] 1: Mat.-Naturvidensk. Kl.* **1926**.

(23) Ertem, G. *Clays Clay Miner.* **1972**, *20*, 199.

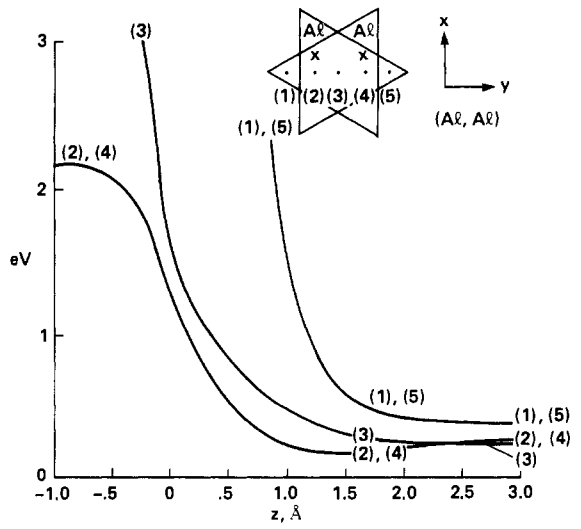

Figure 3. Energy of interaction between a unit positive test charge and the 2:1 layer with no isomorphic substitution along pathways whose projections are displayed in the inset on the upper right. The view is perpendicular to the upper sheet in Figure 1 (the sheet contains atoms 12, 13, ..., 23).

Ca^{2+} seem not to occur naturally. It is clear from the Table II entry under the reaction

$$(Al^{3+},\text{vacant})^{3-} + M^{i+} \rightarrow (Al^{3+},M^{i+})^{i-3}$$

that, if the insertion of the bare K^+ ion into a vacant site is less favorable than the site remaining vacant, then insertion from a hydrated form of K^+ will be even more unfavorable. The Na^+ and Ca^{2+} ions comprise a grouping separate and distinct from the other metal ions in Table II; it follows from the energetics that, if sodium cannot participate in isomorphic substitution, then neither can Ca^{2+}.

The effect of isomorphic substitution on the charge density of the oxygens that are in direct contact with the aqueous interlamellar phase is of interest. Irrespective of the cation substituted for an Al^{3+} ion, we found as a result of our calculations that the charge on these oxygens (labeled 12–23 in Figure 1), which form the boundary of the interlaminar region, does not change by more than 4%. From these calculations we conclude that, in this model system, the excess negative charge is dispersed throughout the crystal and that it was not obvious where the exchangeable cation would be located. It appears, therefore, that the presence of an exchangeable ion in the hydrated interlayer would determine the final electron density patterns, rather than the isomorphically substituted octahedral layer immutably fixing the electronic density pattern.

For a determination of whether the small variations in charge distributions, which were associated with each particular isomorphically substituted metal ion, did translate to an unambiguous effect on an external cation, a positive test charge was introduced. The potential energy of interaction between this charge and the screened charges of the laminar structure (obtained from the IEH calculations) was computed for a range of positions. Polarization effects as well as crystalline repulsion terms were neglected; that is, the calculations were purely electrostatic. The test charge was a bare-point charge; consequently, charge transfer was excluded. The IEH approach tends to minimize charge redistribution, which, in turn, generally eliminates drastic changes in assigned charges. Since the bare-point charge will have no overlap with the orbitals of the crystalline phase, no charge redistribution would

(24) McBride, M. B.; Mortland, M. M. *Soil Sci. Soc. Am. Proc.* **1974**, *38*, 408. Other metal ions besides Li^+ penetrate.

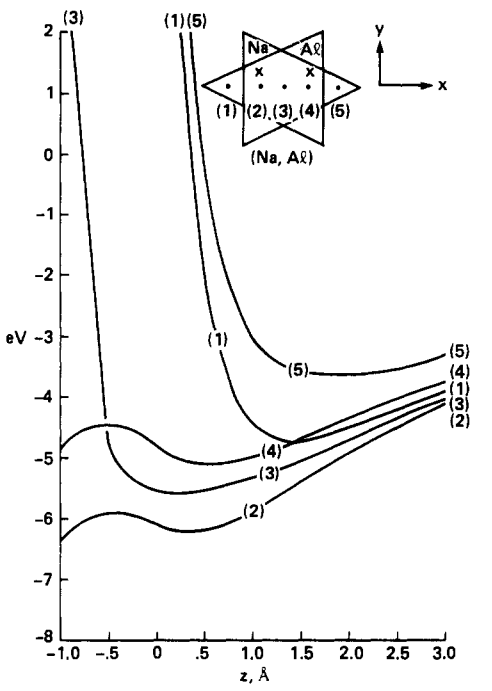

Figure 4. Energy of interaction between a unit positive test charge and the 2:1 layer when sodium has replaced an aluminum ion.

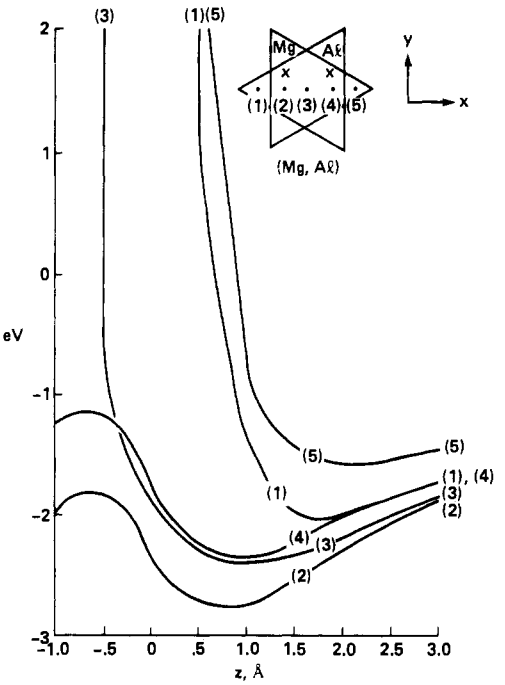

Figure 5. Energy of interaction between a unit positive test charge and the 2:1 layer when a magnesium has replaced an aluminum ion.

be expected from an IEH calculation in any event. Though this is an artifice, the electrostatic results are, within the IEH context, formally exact.

The test charge was brought down along an axis (taken to be the *z* axis) perpendicular to the topmost layer in Figure 1 at five different positions along that face in its idealized hexagonal arrangement. Two pathways (labeled (1) and (5) in Figures 3–7) are through the center of the bases of SiO_4 tetrahedra and ultimately intersect with Si atoms. Another pathway (labeled (3)) would eventually intersect with a hydroxyl group. The remaining two pathways (labeled (2) and (4)) will not intersect with any atom. The test charge was taken to a depth of 1 Å below the surface of the laminar structure (where zero is defined as a plane through the centers

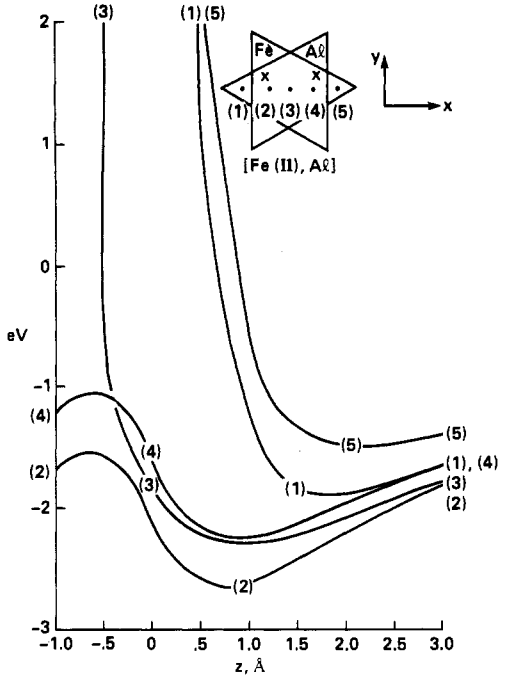

Figure 6. Energy of interaction between a unit positive test charge and the 2:1 layer when a ferrous ion has replaced an aluminum ion.

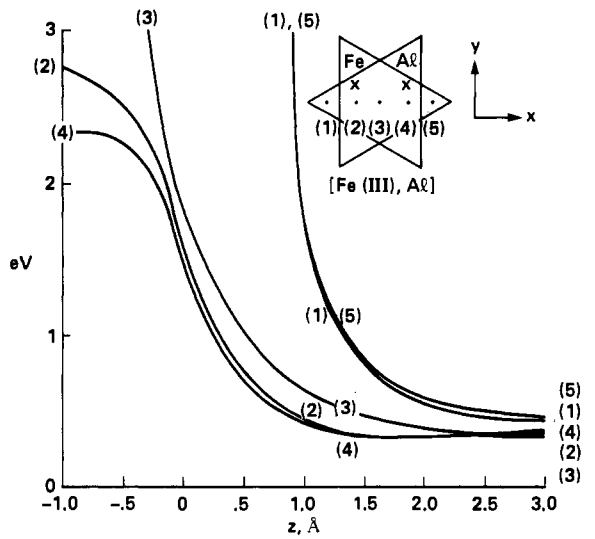

Figure 7. Energy of interaction between a unit positive test charge and the 2:1 layer when a ferric ion has replaced an aluminum ion.

of the surface oxygen nuclei). The curves displayed in Figure 3, for the case in which no isomorphic substitution has occurred, are purely repulsive. Thus there is no stable region (where the potential energy is negative) for an external positive charge for any of the pathways considered. Only three curves are displayed; the environments associated with pathways 1 and 2 are essentially identical with pathways 5 and 4, respectively. Curve 1, 5 and curve 3 will diverge because the test charge's pathways intersect with a Si in the former two cases and the H of an OH group in the latter case. This pattern is *not* observed when an Al^{3+} is replaced by Na^+, K^+, Mg^{2+}, Ca^{2+}, or Fe^{2+}. The curves for Na^+ (Figure 4) are very similar to those for K^+; Mg^{2+} curves (Figure 5) are representative of those obtained with Ca^{2+} as the isomorphically substituted metal ion. For all these isomorphic substituents, all five curves display regions of stability (the potential energy is negative). Curves 2 and 4 for Na^+, Mg^{2+}, and Fe^{2+} (Figures 4–6, respectively) display minima above the surface but possess only a small barrier to penetration into the solid phase by the positive test charge. The heights of these barriers range from 0.3 eV (curve 2, Figure 4) to 1.1 eV (curve 2, Figure 6). Beyond the barrier, there is an attractive region. Hence, we might expect that small positive ions could penetrate into the solid phase of the clay at elevated temperatures for the Mg^{2+} or Fe^{2+} isomorphically substituted clay. Such penetration into the solid phase of some clays has been observed for Li^+.[23,24] Introduction of Fe^{3+} (Figure 7) results in purely repulsive curves similar to the ones in Figure 3. Though the modeling is incomplete, the results are in qualitative agreement with experiment. The expected effect of hydration, from previous work,[12] is to shift equilibrium positions farther from the surface and make penetration into the solid phase more difficult.

In passing, we also examined the relative ease of reducing a ferric ion to the ferrous state in the octahedral environment of montmorillonite clay as compared with the reduction of free, hydrated Fe^{3+}. The free, hydrated state was modeled by disposing six waters about the ferric ion. The oxygens were at the vertices of an octahedron, and the overall symmetry was D_{2h}. An equilibrium configuration was determined by the simultaneous dilation or contraction of the water molecules and calculation of the energy for each configuration. The calculated Fe–O equilibrium distance for either $Fe^{II}{\cdot}6H_2O$ or $Fe^{III}{\cdot}6H_2O$ was 2.8 ± 0.2 Å. We found that

$$\Delta E[Fe^{III}{\cdot}6H_2O + e^- \rightarrow Fe^{II}{\cdot}6H_2O] = +9.3 \text{ eV}$$

On the other hand, with reference to Table II

$$\Delta E[(Al^{3+},Fe^{3+})^0(\text{clay}) + e^- \rightarrow (Al^{3+},Fe^{2+})^-(\text{clay})] = +4.4 \text{ eV}$$

Therefore, we conclude from these results that it is easier to reduce the isomorphically substituted Fe^{3+} than the free, hydrated form; this appears to be in accord with experiment.[25]

Because of computational limitations, the set of atoms used in this study is significantly less than that found in a real clay particle. As a result, *there is no guarantee that we have captured the most significant aspects of clay chemistry.* Therefore, the conclusions must be viewed as correlative and predictive in nature. Since the results reported appear to agree with experimental observation, future studies are warranted.

Our discussion will conclude with consideration of results that are both suggestive and indicative of areas in which further investigation is needed. The molecular orbitals about the Fermi level for the series where an Al^{3+} ion has been isomorphically substituted with Na^+, K^+, Mg^{2+}, Ca^{2+}, Fe^{2+}, Fe^{3+}, or a vacancy are displayed in Figure 2. As noted in the beginning of this section, the nature of the topmost filled orbitals does not change drastically regardless of the specific cation in the octahedral site. These topmost orbitals are basically centered on oxygens composing the octahedral layer framework. The filled orbitals are pushed up with respect to the valence band for all the isomorphic substitutional cases considered. Similarly, the lowest empty orbitals are interspersed in a conduction band. While we have adopted solid-state terminology in describing a miniscule model system, we believe that the results are indicative of limit behavior. Thus, with reference to Figure 2, the montmorillonite will display properties reminiscent of a semiconductor. The topmost filled orbitals are essentially localized in regions about specific octahedral sites, and the conduction-band molecular orbitals are diffuse. Hence promotion of an electron from a localized site to the conduction band affects the entire system. How this behavior might translate into catalytic properties remains to be determined.

Registry No. Al^{3+}, 22537-23-1; Na^+, 17341-25-2; K^+, 24203-36-9; Mg^{2+}, 22537-22-0; Ca^{2+}, 14127-61-8; Fe^{2+}, 15438-31-0; Fe^{3+}, 20074-52-6; montmorillonite, 1318-93-0.

(25) Banin, A. Professor, Hebrew University, Israel, private communication.